Text and references for Nevada Bureau of Mines and Geology Map 144

GEOLOGIC MAP OF THE MULE CANYON QUADRANGLE

LANDER COUNTY, NEVADA

by

David A. John and Chester T. Wrucke

INTRODUCTION

The Mule Canyon Quadrangle covers about 145 km^2 of the northwest end of the Shoshone Range, including the west ends of the Argenta and Malpais rims, in northern Lander County, Nevada, about 20 km southeast of Battle Mountain (fig. 1). The Shoshone Range is a long north-northeast-trending range formed by late Cenozoic high-angle normal faulting related to basin-and-range extension. The Argenta and Malpais rims are short, northeast- to east-northeast-trending ridges with steep north sides and shallow south-facing dip slopes. They formed by dominantly dip-slip, left-lateral oblique-slip faulting also related to late Cenozoic (post-late Miocene) basin-and-range extension (Zoback and others, 1994). The west end of Whirlwind Valley lies between the Argenta and Malpais rims on the east side of the Mule Canyon Quadrangle (fig. 1). Geology of most of the Mule Canyon Quadrangle was mapped by D.A. John and C.T. Wrucke of the U.S. Geological Survey in 1996–2002. This mapping was combined by D.A. John with a more detailed (1:12,000), unpublished geologic map of the central part of the quadrangle by T.A. Chapin completed in 1992 for Gold Fields Mining Corp. (see source of geologic mapping).

GEOLOGY

The Mule Canyon Quadrangle includes rocks ranging in age from lower Paleozoic to middle Miocene that are covered locally by Quaternary surficial deposits (fig. 2). The western third of the quadrangle is underlain by lower Paleozoic siliciclastic sedimentary rocks of the Roberts Mountains allochthon that are overlain unconformably by early Oligocene to early Miocene sedimentary and volcanic rocks. These rocks are overlain unconformably and intruded by middle Miocene igneous rocks related to the north-northwest-trending northern Nevada rift (Zoback and Thompson, 1978; Zoback and others, 1994; John and others, 2000), the western margin of which passes through the center of the quadrangle (figs. 1 and 2). The middle Miocene igneous rocks underlie the central and eastern parts of the quadrangle and host epithermal gold-silver deposits at the Mule Canyon Mine in the north-central part of the quadrangle.

ROCK UNITS

Paleozoic Sedimentary Rocks

Lower Paleozoic sedimentary rocks of the Roberts Mountains allochthon crop out along the west flank of the northern Shoshone Range (Stewart and McKee, 1977). Exposed along the west side of the Mule Canyon Quadrangle, the Paleozoic rocks consist of the Cambrian-Ordovician Valmy Formation, the Silurian-Devonian Elder Sandstone, and the Devonian Slaven Chert. The Paleozoic rocks are imbricated by low-angle faults, probably thrust faults formed during the Late Devonian to Early Mississippian Antler orogeny (Roberts and others, 1958). Cross sections A–A´ and B–B´ illustrate the probable configuration of these rocks and faults.

The Valmy Formation (O€vu) forms two thrust sheets separated by a thrust sheet of Slaven Chert. The lower thrust sheet is composed of interbedded quartzite and argillite and minor limestone, whereas the upper thrust sheet is composed mostly of quartzite. Black to medium-gray argillite (Ova) forms a thin thrust sheet at the base of the lower thrust sheet, and small lenses of greenstone (Ovg) are present in two localities. Graptolites from fossil localities F3, F8, F9, and F10 in the northwestern part of the map indicate a Late Ordovician age (table 2); the Cambrian age is based on very late Late Cambrian conodont elements from limestone in the Valmy Formation in the Stony Point Quadrangle 1 km north-northwest of the northwest corner of the Mule Canyon Quadrangle (A.G. Harris, written commun., 1998). The argillite unit has an Early or Middle Ordovician age based on graptolites at fossil locality F4 (table 2).

The Elder Sandstone (Se) is recognized only in one small fault block in the west-central part of the quadrangle. It consists of dark-gray to black shale, siltstone, and laminated silty limestone. It structurally overlies the Slaven Chert and is faulted against quartzite of the Valmy Formation. Graptolites found in shale at locality F7 are upper Early Silurian (upper Wenlockian) in age (table 2). Elsewhere in northern Nevada, the age of the Elder Sandstone extends into the Early Devonian (Noble, 2000).

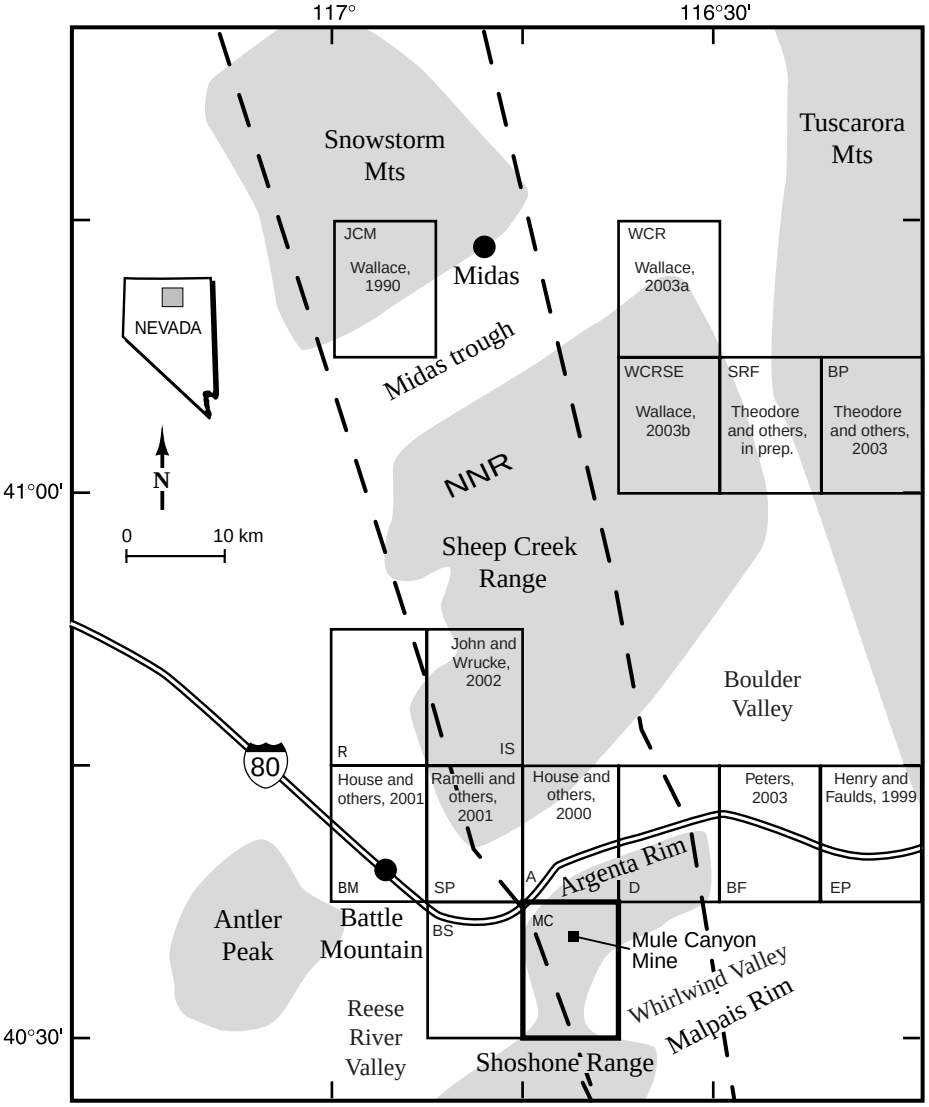

Figure 1. Index map showing location of Mule Canyon 7½-minute Quadrangle (MC), recent geologic maps, geographic features mentioned in text, and approximate outline of northern Nevada rift (NNR). 7½-minute quadrangles: A, Argenta; BF, Bobs Flat; BM, Battle Mountain; BP, Beaver Peak; BS, Bateman Spring; D, Dunphy; EP, Emigrant Pass; IS, Izzenhood Spring; JCM, Jake Creek Mountain; R, Russells; SP, Stony Point; SRF, Santa Renia Fields; WCR, Willow Creek Reservoir; WCRSE, Willow Creek Reservoir SE.

The Slaven Chert (Dsc) is exposed in two major thrust sheets separated by a thrust sheet of the Valmy Formation. The Slaven Chert consists of gray to black ribbon chert, fine-grained sandstone and quartzite, argillite, siltstone, calcareous sandstone, bedded barite, and minor greenstone. The lower thrust sheet contains numerous conspicuous sandstone and quartzite sequences. The higher thrust sheet contains medium- to dark-gray barite in beds 1 to 30 cm thick, locally in sequences as thick as 5 m with interlayered chert. Fossils in the lower thrust sheet at fossil localities F1, F2, and F5 are Early Devonian (table 2). The age of the upper thrust sheet is possibly Early to Late Devonian; a Middle Devonian age was determined from conodonts obtained in this quadrangle at fossil locality F11 (table 2) in the southwestern part of the map area.

In the west-central part of the quadrangle, large exposures of fine-grained feldspathic sandstone and siltstone (Dss) overlie typical Slaven Chert and are tentatively correlated with similar dated rocks in the southwestern Sheep Creek Range to the north and in the Tenabo area farther to the south in the Shoshone Range (House and others, 2001; C.T. Wrucke, unpub. data, 2002). The age of Dss is uncertain, but it overlies chert of early Middle Devonian age at fossil locality F11 (table 2). Along the west border of the quadrangle, the upper part of the Slaven Chert is interbedded locally with medium-grained sandstone commonly containing several percent of sand and grit-size fragments of black chert (Dssc). Sandstone commonly is interlayered with abundant chert breccia consisting of pebble-size, black to medium-gray fragments of chert. Chert clasts are dominantly angular but some are rounded to subrounded. The sandstone and chert breccia unit locally contains thin lenses of dark gray limestone. This unit has an Early Devonian age on the basis of its position between fossil localities F1 and F2 (table 2).

Early Oligocene Caetano Tuff

Crystal-rich rhyolite ash-flow tuff that we correlate with the regionally widespread early Oligocene Caetano Tuff (Gilluly and Masursky, 1965; Stewart and McKee, 1977) locally unconformably overlies the Paleozoic rocks along the west side of the Mule Canyon Quadrangle. This tuff

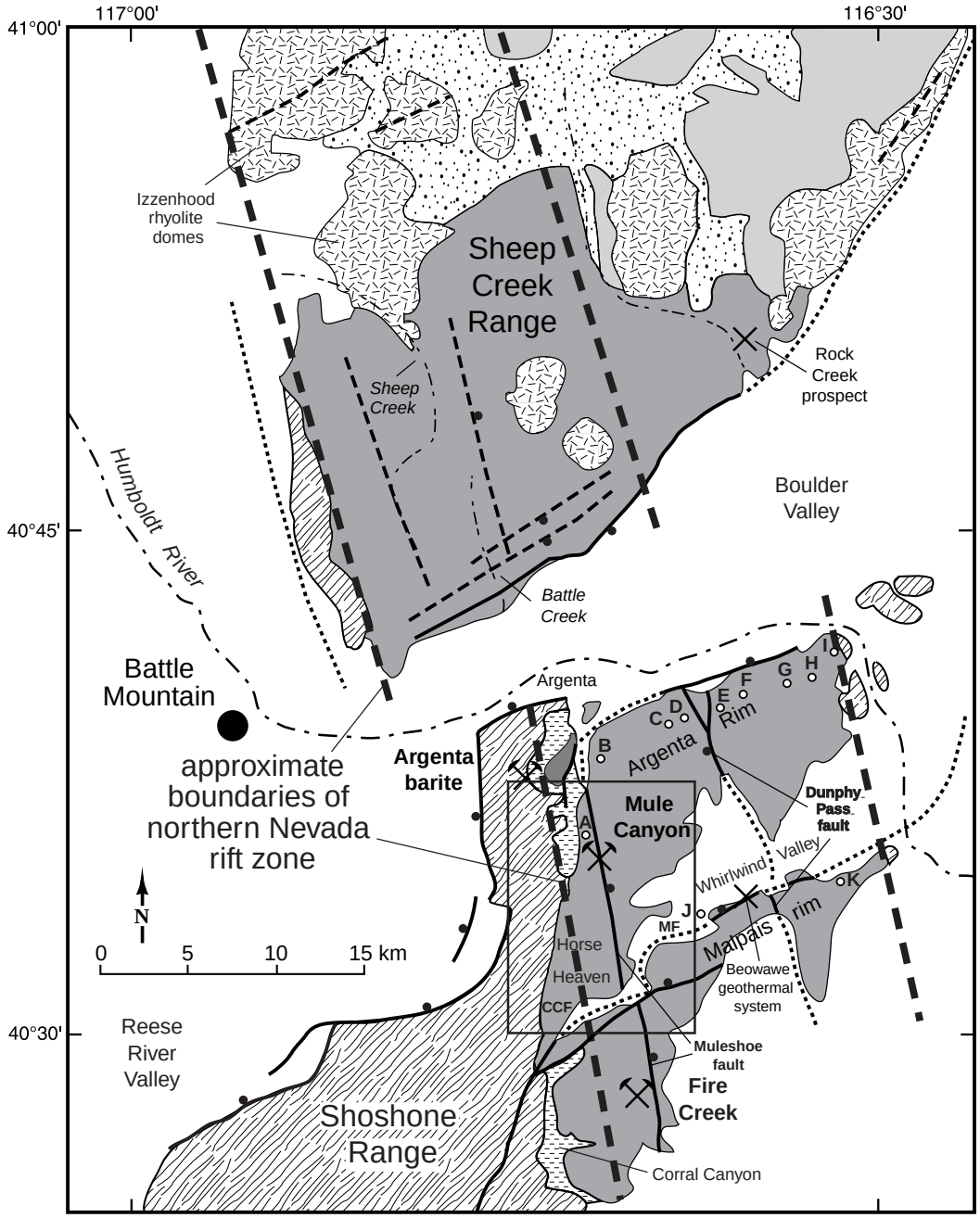

EXPLANATION

- Younger alluvium (Quaternary)
- Older alluvium (Quaternary and late Tertiary)
- Younger sedimentary rocks (Miocene)
- Rhyolite (Miocene)
- Basalt, andesite, and dacite (Miocene)
- Older sedimentary rocks (Oligocene and/or Miocene)
- Sedimentary rocks (Paleozoic)
- Faults, dashed where approximately located, dotted where concealed. Ball on downthrown side
- Approximate structural margin of northern Nevada rift zone
- F — Location of stratigraphic sections (fig. 3)

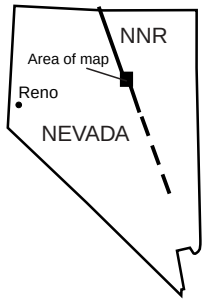

Figure 2. Generalized geologic map of the northern Shoshone Range, the Argenta and Malpais Rims, and the southern Sheep Creek Range, Nevada, showing location of the Mule Canyon and Fire Creek deposits and the Beowawe geothermal system and approximate locations where stratigraphic sections were determined (fig. 3). Box shows location of the Mule Canyon 7½-minute Quadrangle. Small map shows location of figure and heavy line shows trace of the northern Nevada rift (NNR). Geology modified from Stewart and McKee (1977) and Stewart and Carlson (1976). CCF, Corral Canyon fault; MF, Malpais fault.

Table 1. $^{40}Ar/^{39}Ar$ dates of igneous rocks from the northern Shoshone and southwestern Sheep Creek Ranges, Nevada

Map No.	Sample No.	Rock Type (map unit)	Material Dated	Type of Analysis[1]	Date ±1σ (Ma)[2]	Comments	Latitude	Longitude
Northern Shoshone Range								
A1	979-17G	Basalt (Tob)	whole rock	IH	14.7±0.8	Capping olivine basalt lava flow east of Mule Canyon Mine	40°35'19"N	116°39'38"W
A2	96-MC-48b	Dacite (Tpd)	plagioclase	IH	15.33±0.09	Lava flow just east of Main pit	40°35'08"	116°40'33"
A3	99-MC-4b	Quartz vein	adularia	LF	15.59±0.04	Electrum-bearing vein, South pit, Mule Canyon Mine	40°35'13"	116°41'08"
A4	99-DJ-99	Andesite (Thh)	whole rock	IH	15.86±0.12	Andesite of Horse Heaven	40°33'19"	116°41'55"
A5	98-DJ-71	Andesite (Thh)	whole rock	IH	15.2±0.8	Andesite of Horse Heaven	40°32'27"	116°42'13"
A6	979-17C	Andesite (Tba)	whole rock	IH	15.85±0.08	Andesite flow	40°35'51"	116°41'20"
A7	00-MC-44	Basalt (Tmc)	whole rock	IH	15.91±0.09	Lava flow in middle of Mule Canyon sequence, Northwest pit, Mule Canyon Mine	40°35'58"	116°41'22"
--	99-VB-66b	Basaltic andesite (Tbi)	whole rock	IH	16.13±0.09	Dike intruded into Slaven Chert in Argenta barite mine	40°38'04"	116°43'42"
A8	99-DJ-95	Basaltic andesite (Tbi)	whole rock	IH	16.4±0.4	Dike intruding Tertiary sedimentary rocks 3 km SW of Mule Canyon Mine	40°34'06"	116°42'30"
A9	98-DJ-52	Rhyolite tuff (Tct)	sanidine	LF	33.87±0.08	Basal vitrophyre of Caetano Tuff	40°31'20"	116°43'01"
A10	H00-53	Rhyolite tuff (Tct)	sanidine	LF	34.01±0.04	Devitrified Caetano Tuff	40°34'10"	116°42'38"
Southwestern Sheep Creek Range								
--	97-DJ-56	Basalt (Tob)	whole rock	IH	14.7±0.2	Capping olivine basalt flow	40°45'41"	116°45'29"
--	979-17I	Rhyolite porphyrys	anidine	LF	14.84±0.04	Basal vitrophyre from coarsely porphyritic rhyolite flow	40°51'22"	116°50'06"
--	97-DJ-55	Rhyolite tuff	sanidine	LF	14.94±0.04	Air-fall tuff underlying olivine basalt (sample 97-DJ-56)	40°45'20"	116°45'46"
--	979-17H	Dacite (Tpd)	plagioclase	IH	15.34±0.10	Vitrophyric porphyritic dacite	40°50'25"	116°51'31"
--	979-17J	Trachydacite (Td)	plagioclase	IH	15.42±0.10	Flow banded trachydacite lava underlying rhyolite porphyry (sample 979-17I)	40°51'19"	116°50'14"
--	979-17K	Basalt (Tob)	whole rock	IH	15.58±0.10	Basal basalt flow unconformably overlying Paleozoic sedimentary rocks	40°43'26"	116°50'36"
Corral Canyon, Shoshone Range (fig. 2)								
--	99-DJ-61	Andesite (Thh)	whole rock	IH	15.76±0.80	Andesite of Horse Heaven	40°26'08"	116°40'18"

[1]LF, laser fusion, weighted mean age; IH, incremental heating

[2]Irradiation flux for all samples except H00-53 was monitored by use of 85G003 Taylor Creek Rhyolite sanidine standard, which has an age of 27.92 Ma relative to an assigned age of 513.9 Ma for MMhb-1 hornblende. Sample H00-53 (A10) was analyzed by Chris Henry, Nevada Bureau of Mines and Geology, at the New Mexico Geochronology Research Laboratory, New Mexico Bureau of Geology and Mineral Resources. The flux monitor for that analysis was Fish Canyon Tuff sanidine, which has an age of 27.84 Ma relative to an assigned age of 520.4 Ma for MMhb-1. Fish Canyon

forms steep east-dipping erosional remnants that may have been deposited in a north-trending paleovalley. The tuff is believed to have been erupted from a caldera source on the northwest side of the Cortez Range about 50 km to the southeast (Stewart and McKee, 1977), although Wrucke and Silberman (1975) suggested that a deeply eroded caldera at Mount Lewis in the northern Shoshone Range was another possible source of this tuff. Sanidine from the the tuff exposed the quadrangle yielded $^{40}Ar/^{39}Ar$ dates of 33.87±0.08 and 34.01±0.04 Ma (A9 and A10, table 1).

Middle Tertiary Sedimentary Rocks

Fine- to coarse-grained clastic sedimentary rocks and minor limestone unconformably overlie the Paleozoic rocks and the Caetano Tuff along the west side of the Mule Canyon Quadrangle. In the northwest part of the quadrangle, the lower part of this sequence commonly consists of pebble to boulder conglomerate and sedimentary breccia (unit Tc) that contains rounded clasts of Paleozoic rocks and blocks of the Caetano Tuff as much as several meters wide and a lens of brecciated Caetano Tuff about 200 m long. The conglomerate also contains sparse clasts of sparsely porphyritic rhyolite ash-flow tuffs that may correlate the regionally extensive units B and D of the Bates Mountain Tuff (C.D. Henry, oral commun., 2003). These rocks probably are fluvial and alluvial-fan deposits. Most of the Tertiary sedimentary rocks (unit Ts) are composed of fine-grained siltstone, shale, and mudstone, with sparse beds of ostracode-bearing limestone. These rocks probably were deposited in a lacustrine environment. The sedimentary rocks form a sequence that generally fines upward from coarse conglomerate and breccia to finely laminated mud and chemical sediment. Exposures of the sedimentary rocks near the southwest corner of the quadrangle also contain thin beds of reworked pyroxene-rich mafic tuff that may represent early eruptions of mafic rocks related to the middle Miocene northern Nevada rift. The sequence probably was deposited along the west side and near the north end of a north- to northwest-elongated basin that extended from the Humboldt River on the north side of the Shoshone Range about 75 km to the Simpson Park Range to the south along the axis of the future northern Nevada rift, as suggested by discontinuous exposures of classic sedimentary rocks directly beneath middle Miocene mafic volcanic rocks related to the northern Nevada rift throughout this area (fig. 1; John and others, 2000). The age of these sedimentary rocks is bracketed between the age of the underlying Caetano Tuff (about 34 Ma) or Bates Mountain Tuff (about 28 to 25 Ma) and the age of dikes that intrude the sedimentary rocks (about 16.4 Ma; table 1). The presence of hyaloclastic breccias at the base of the overlying Mule Canyon sequence suggest that these rocks were erupted onto wet sediments or water and that the uppermost sediments are likely middle Miocene. This age also is suggested by the local presence of mafic tuffs possibly related to the northern Nevada rift in the upper part of this unit.

Middle Miocene Igneous Rocks

Middle Miocene igneous rocks unconformably overlie and intrude the Paleozoic and middle Tertiary rocks, capping the north end of the Shoshone Range and the Argenta and Malpais rims (fig. 1). These rocks formed along the northern Nevada rift, which extends 500 km from the Oregon-Nevada border to southeast Nevada, and was the site of middle Miocene continental rifting, igneous activity, and related precious-metal mineralization (Zoback and others, 1994; Wallace and John, 1998; John and others, 2000).

In the Mule Canyon Quadrangle, the middle Miocene extrusive rocks include (1) early mafic rocks including of the Mule Canyon sequence (unit Tmc), basalt and andesite (unit Tba), and andesite of Horse Heaven (unit Thh), (2) porphyritic dacite (unit Tpd) and trachydacites (unit Td), and (3) capping olivine basalt (unit Tob). In addition, numerous dikes and irregular intrusive bodies, mostly of fine-grained basalt and basaltic andesite (unit Tbi), are exposed in the northwest quarter of the quadrangle. These dikes intruded the pre-middle Miocene rocks and locally intruded and fed the Miocene lava flows. $^{40}Ar/^{39}Ar$ dating indicate that all these units formed between about 16.4 and 14.7 Ma (table 1).

Early mafic rocks

Mafic rocks, consisting of basalt to andesite lava flows, dikes, irregular intrusions, and minor pyroclastic rocks, are the oldest middle Miocene rocks and crop out extensively in the central third of the quadrangle. These rocks are divided into four map units: Mule Canyon sequence, basalt and andesite, andesite of Horse Heaven, and basalt and basaltic andesite intrusive rocks.

The Mule Canyon sequence (unit Tmc) unconformably overlies the middle Tertiary sedimentary and volcanic rocks and Paleozoic sedimentary rocks along the west side of the quadrangle. On the basis of extensive drilling data in the Mule Canyon Mine area, this sequence consists of as many as 15 distinct units with an aggregate thickness of about 400 m in the mine area (Thomson and others, 1993; Newmont Gold Co., 1999; John and others, 2003). The uppermost unit in this sequence, the basalt and andesite unit (Tba), is shown separately on the geologic map, because it was mapped consistently as a separate unit by mining company geologists (flow banded basalt unit, Thomson and others, 1993; Newmont Gold Co., 1999; John and others, 2003). The Mule Canyon Mine area was an eruptive center for the Mule Canyon sequence, and several vents for the upper parts of the sequence are exposed in the open-pit mines (Newmont Gold Co., 1999; John and Wallace, 2000). Drill-hole data indicate that the Mule Canyon sequence rapidly thins to the south from about 400 m in the mine area to less than 100 m near the south end of the quadrangle, and many units that are present in the mine area are absent farther south. Drill-hole data from the Beowawe geothermal area (fig. 1; Struhsacker, 1980) and reconnaissance mapping of

Table 2. Biostratigraphic information for the Mule Canyon Quadrangle, Nevada

Locality Number	UTM East UTM North	Field No., (USGS Collection No.)	Stratigraphic Unit	Fauna	Age	Source
F1	522,123 4,494,433	01-DJ-08 (12769-SD)	Slaven Chert (Dsc)	Conodonts: *Belodella* sp. *Dvorakia* sp. Icriodontid elements *Ozarkodina pandora* Murphy, Matti, and Walliser beta morphotype *Ozarkodina pandora* Murphy, Matti. A md Walliser mu morphotype? *Ozarkodina* spp. *Panderodus* sp. *Polygnathus* sp. *Pseudooneotodus beckmanni* (Bischoff and Sannemann) Redeposited Ordovician conodonts: *Periodon aculeatus* Hadding (early-middle Middle Ord.) prioniodontid elements	middle Early Devonian (likely middle to late Pragian)	Anita G. Harris[1] written commun., 2001
F2	521,915 4,494,137	MC 70 (12633-SD)	Slaven Chert (Dsc)	Conodonts: *Bellodella* sp. *Ozarkodina excavata* (Branson And Mehl) *Ozarkodina* spp. *Panderodus* sp. *Pseudooneotodus beckmanni* (Bischoff and Sannemman)	Early Devonian but not latest Early Devonian	Anita G. Harris[1] written commun., 2001
F3	523,500 4,493,690	SHO-99-25	Valmy Formation, undivided (O€vu)	Graptolites: *Normalograptus tubuliferus* *Reteogrptus pucherrimus* *Dicellograptus* sp. *Climacograptus* sp.	latest Ordovician	S.C. Finney[2] (J.K. Cluer, written commun., 2001)
F4	521,572 4,492,835	01-DJ-01	Valmy Formation, argillite (Ova)	Graptolite: Uniserial stipe fragment with dichograptid thecae. Specimen too incomplete for species identification.	Ordovician, probably Early to Middle Ordovician, but very uncertain	S.C. Finney[2] written commun., 2001
F5	521,469 4,494,500	01-DJ-02 (12768-SD)	Slaven Chert, sandstone and chert breccia (Dssc)	Conodonts: *Belodella* sp. *Dvorakia* sp. *Icriodus* sp. *Ozarkodina excavata* (Branson and Mehl) *Panderodus unicostatus* (Branson and Mehl) *Pseudooneotodus beckmanne* (Bischoff and Sannemann)	Early Devonian (Lochkovian-early Emsian), no younger than early late Early Devonian	Anita G. Harris[1] written commun., 2001

continued

Table 2. Biostratigraphic information for the Mule Canyon Quadrangle, Nevada (*continued*)

Locality Number	UTM East UTM North	Field No., (USGS Collection No.)	Stratigraphic Unit	Fauna	Age	Source
F6	521,580 4,492,370	SHO-99-18	Slaven Chert, sandstone and chert breccia (Dssc)	Conodonts: *Icriodus steinachensis* *Ozarkodina "linearis"* (philip) *Pseudooneodotus beckmanni* Palmatolepis *sp*.	Early to Late Devonian	M.T. Kurka[3] (J.K. Cluer, written commun., 2001)
F7	523,677 4,491,313	01-DJ-03	Elder Sandstone (Se)	Graptolite: *Pristograptus dubius*	upper Early Silurian (upper Wenlockian)	S.C. Finney[2] written commun., 2001
F8	521,167 4,490,136	SHO-99-12	Valmy Formation, undivided (O€vu)	Graptolites: *Normalograptus* sp. (*brevis eugluphus*, or *tubuliferous*) *Pseudoclimacograptus* ?*Orthograptus quadrimucronatus* group?	early Late Ordovician	S.C. Finney[2] (J.K. Cluer, written commun., 2001)
F9	521,350 4,490,170	SHO-99-13	Valmy Formation, undivided (O€vu)	Graptolite: *Climacograptus* sp.	Probably Late Ordovician	S.C. Finney[2] (J.K. Cluer, written commun., 2001)
F10	521,510 4,490,080	SHO-99-14	Valmy Formation, undivided (O€vu)	Graptolites: ?*Pseudoclimacograptus* ?*Glyptograptus* or ?*Orthograptus* *Normalograptus* or ?*brevis* or ?*euglyphus* ?*Lasiograptus* or ?*Pseudoclimacograptus* *Leptograptus* or *Dicellograptus* stipe fragment *Glossograptus* sp.	early Late Ordovician	S.C. Finney[2] (J.K. Cluer, written commun., 2001)
F11	521,710 4,486,880	SHO-99-32	Slaven Chert (Dsc)	Conodont: Rare *Trilonche* fragments *Ceratoikiscum calvum*	early Middle Devonian (Eifelian) or slightly older	P.J. Noble[3] (J.K. Cluer, written commun., 2001)

[1]U.S. Geological Survey, Reston, Virginia 20192
[2]Department of Geological Sciences, California State University - Long Beach, Long Beach, California 90840
[3]Department of Geological Sciences, University of Nevada, Reno, Nevada 89557

Argenta Rim (fig. 3; John and others, 2000) indicate that the Mule Canyon sequence extends east of the quadrangle and is several hundred meters thick in the Whirlwind Valley area. The middle and upper parts of the Mule Canyon sequence are the principal host rocks for gold ore at the Mule Canyon Mine.

Several units in the Mule Canyon sequence contain textures suggesting eruption into water or onto water-saturated rocks. These include hyaloclastic breccias locally exposed at the base of the sequence, vague pillow shapes of quenched, glassy basalt flows, and palagonitized basalt flows. Quenched basalt dikes with brecciated, perlitic margins also suggest emplacement into water or water-saturated rocks (see below).

Rocks in the Mule Canyon sequence range in composition from basalt to andesite (fig. 5 and table 3; John and others, 2000). A whole-rock $^{40}Ar/^{39}Ar$ date of 15.91±0.09 Ma was obtained on a basalt flow in the middle of the sequence, and the overlying basalt and andesite unit yielded a whole-rock date of 15.85±0.08 Ma (A7 and A6, respectively, table 1).

The andesite of Horse Heaven conformably overlies the Mule Canyon sequence. It is a widely distributed sequence of sparsely porphyritic andesite and basaltic andesite lava flows that is as much as 250 m thick along the crest of the Shoshone Range a few kilometers south of the Mule Canyon Quadrangle, generally 50–100 m thick in the southwest part of the quadrangle, and thins to ≤40 m in the Mule Canyon Mine area. In the Mule Canyon Quadrangle, the unit consists of as many as eight thin flows marked by highly vesicular, glassy flow tops and massive, holocrystalline flow interiors. Interiors of flows commonly weather spheroidally. Several feeder dikes for the flows are exposed in the Mule Canyon Mine, notably in the Main and Northwest pits (fig. 4; Newmont Gold Co., 1999). Whole-rock samples collected in the south-central part of the Mule Canyon Quadrangle yielded $^{40}Ar/^{39}Ar$ dates of 15.86±0.12 Ma and 15.2±0.8 Ma (A5 and A6, table 1), and a sample collected in Corral Canyon 20 km to the south (fig. 2) yielded a whole-rock date of 15.76±0.80 Ma (table 1; John and others, 2000).

Numerous steeply dipping, north- to north-northwest-striking mafic dikes and large intrusive masses are exposed in the northwestern part of the quadrangle, notably in the open pits of the Mule Canyon Mine. Two ages and types of dikes and intrusions are present in the quadrangle. Many dikes and most large masses intrude lower Paleozoic and middle Tertiary rocks on the west side of the crest of the Shoshone Range. These rocks are mostly fine-grained, equigranular, holocrystalline basaltic andesite that generally is not hydrothermally altered (unit Tbi). Samples of these dikes that intrude lower Paleozoic rocks in the Argenta barite mine 4 km northwest of the Mule Canyon Mine and middle Tertiary sedimentary rocks 3 km southwest of the mine yielded whole-rock $^{40}Ar/^{39}Ar$ dates of 16.13±0.09 and 16.4±0.4 Ma, respectively (table 1).

A second set of basalt to andesite dikes is exposed locally on the west side of the range and more extensively in the Mule Canyon Mine. Many of these dikes have brecciated, glassy (perlitic) margins. The brecciated, glassy dike margins commonly are hydrothermally altered and often form Au-Ag ore. These dikes, and faults along which the dikes were emplaced, commonly channeled hydrothermal fluids that formed ores in the Mule Canyon Mine at about 15.6 Ma (John and others, 2000, 2003). These dikes, most of which were not exposed prior to mining and are not shown on the geologic map, intrude the middle and upper parts of the Mule Canyon sequence and fed some of the upper units in that sequence and in the overlying andesite of Horse Heaven. These relations suggest that these dikes are about 15.8 Ma.

Dacite and trachydacite lava flows

The early mafic rocks are overlain unconformably by thick flows of porphyritic dacite and trachydacite, mostly east of the Muleshoe fault in the east part of the Mule Canyon Quadrangle. These flows extend east across the northern Nevada rift, where they form much of the Argenta and Malpais rims, and similar flows crop out north of the Humboldt River in the southwestern Sheep Creek Range (fig. 2; Struhsacker, 1980; Thomson and others, 1993; John and others, 2000; Ramelli and others, 2001; John and Wrucke, 2002). The dacites thicken toward, and in part are intrusive in, the southwestern Sheep Creek Range, indicating that most of them may have been erupted from there (John and others, 2000; John and Wrucke, 2002).

Two thick flows of porphyritic dacite (unit Tpd) form the lower part of the sequence in the northern Shoshone Range and along the Argenta and Malpais rims. The upper parts of these flows are black vitrophyres that grade downward into irregular zones of spherulitic devitrification characterized by abundant reddish-brown spherulites 0.5 to 6 cm wide. The spherulitic zones grade downward into massive, dark-red to lavender-gray, devitrified dacite. The dacite generally contains 5 to 20 % phenocrysts that consist of plagioclase, clinopyroxene, ilmenite, and minor olivine. The phenocrysts range in size from 0.1 to 4 mm but are mostly <1 mm. They commonly form small glomeroporphyritic clots. Plagioclase phenocrysts yielded $^{40}Ar/^{39}Ar$ dates of 15.33±0.09 and 15.34±0.10 Ma for samples collected in the Mule Canyon Mine and in the southwestern Sheep Creek Range, respectively (table 1).

The porphyritic dacite unit is overlain by a series of trachydacite lava flows that form much of the crest of the Argenta Rim (unit Td). This unit consists of aphyric to sparsely porphyritic flows that contain 1 to 2 % fine- to medium-grained plagioclase, clinopyroxene, ilmenite, and sparse sieve-textured sanidine phenocrysts in a trachytic to pilotaxitic groundmass of plagioclase and Fe-Ti oxide minerals. The flows are marked by glassy, highly vesicular flow tops and devitrified, massive flow interiors that commonly have platy jointing. Vesicles in the flow tops commonly are elongated, forming narrow tubes several centimeters long. The flows are seldom more than about 100 m thick in the Mule Canyon Quadrangle and along the Argenta Rim, and are less than 10 m thick on the Malpais

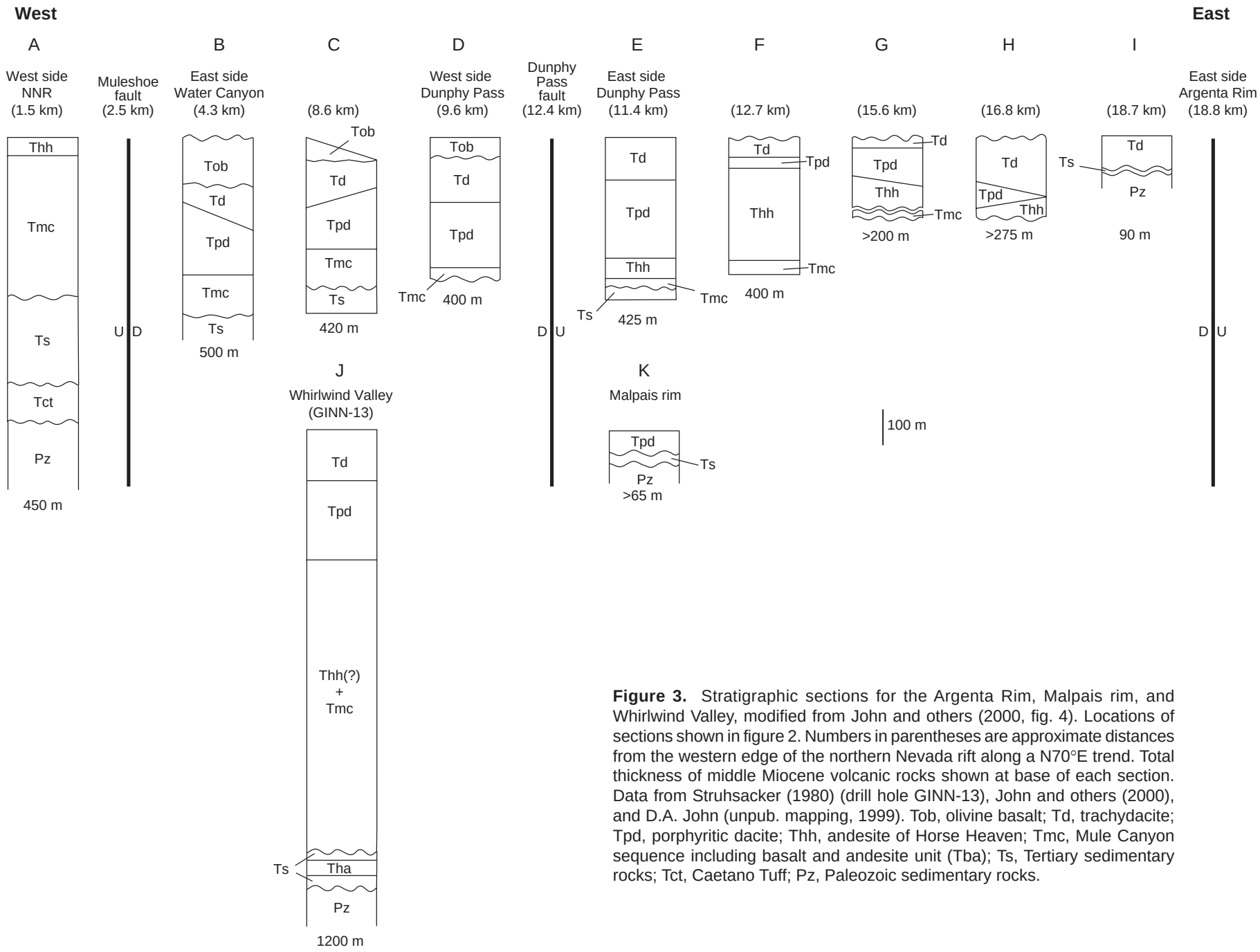

Figure 3. Stratigraphic sections for the Argenta Rim, Malpais rim, and Whirlwind Valley, modified from John and others (2000, fig. 4). Locations of sections shown in figure 2. Numbers in parentheses are approximate distances from the western edge of the northern Nevada rift along a N70°E trend. Total thickness of middle Miocene volcanic rocks shown at base of each section. Data from Struhsacker (1980) (drill hole GINN-13), John and others (2000), and D.A. John (unpub. mapping, 1999). Tob, olivine basalt; Td, trachydacite; Tpd, porphyritic dacite; Thh, andesite of Horse Heaven; Tmc, Mule Canyon sequence including basalt and andesite unit (Tba); Ts, Tertiary sedimentary rocks; Tct, Caetano Tuff; Pz, Paleozoic sedimentary rocks.

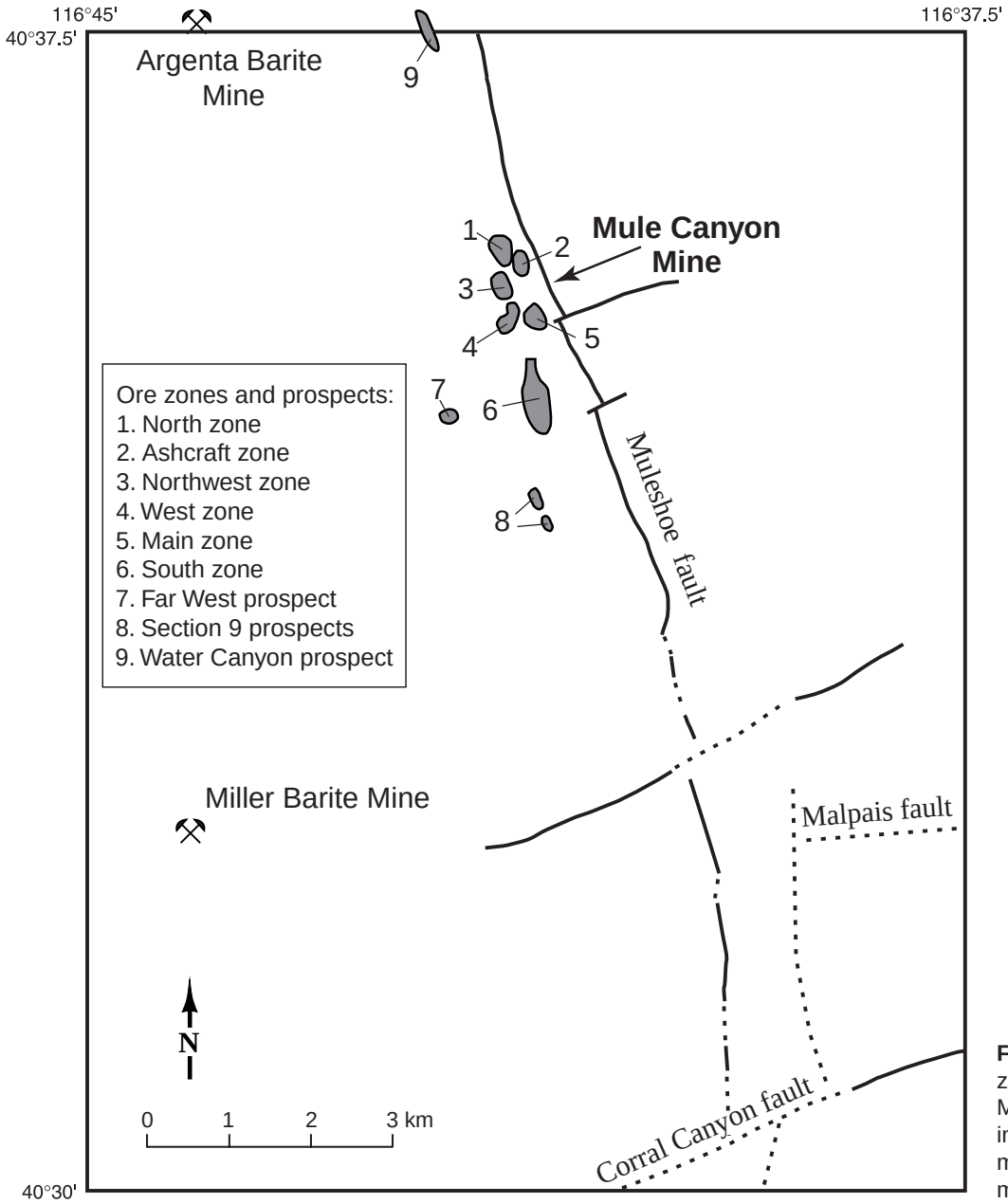

Figure 4. Locations of ore zones at the Mule Canyon Mine, adjacent gold prospects in Miocene rocks, major barite mines in Paleozoic rocks, and major faults.

rim. They thicken to ≥500–600 m in the central part of Izzenhood Spring Quadrangle in the southwestern Sheep Creek Range, suggesting that their source is in the Sheep Creek Range (fig. 1; John and others, 2000; John and Wrucke, 2002). John and others (2000) reported a plagioclase $^{40}Ar/^{39}Ar$ date of 15.42±0.10 Ma on a lava flow collected in the southwestern Sheep Creek Range (table 1).

Capping basalt flows

The northeast part of the Mule Canyon Quadrangle is underlain by olivine basalt lava flows that form dip slopes on the south side of the Argenta Rim. Two thick flows are present in most exposures and have a maximum total thickness of about 130 m just east of the Muleshoe fault along the west end of the Argenta Rim. The two flows locally are separated by <1 m of orange-colored, medium-grained volcaniclastic sandstone on Argenta Rim. The flows contain scattered, small (<2 mm) olivine phenocrysts in a fine-grained, subophitic groundmass of plagioclase, clinopyroxene, and ilmenite. Abundant, very fine-grained cavities are present, producing a spongy, diktytaxitic texture. Petrographically and compositionally identical basalt flows locally form a dip slope on the Malpais rim (Struhsacker, 1980) and similar flows crop out in the southwestern Sheep Creek Range (Ramelli and others, 2001; John and Wrucke, 2002) and extend northward about 45 km to near the intersection of Antelope and Rock Creeks. John and others (2000) reported whole-rock $^{40}Ar/^{39}Ar$ dates of 14.7±0.8 and

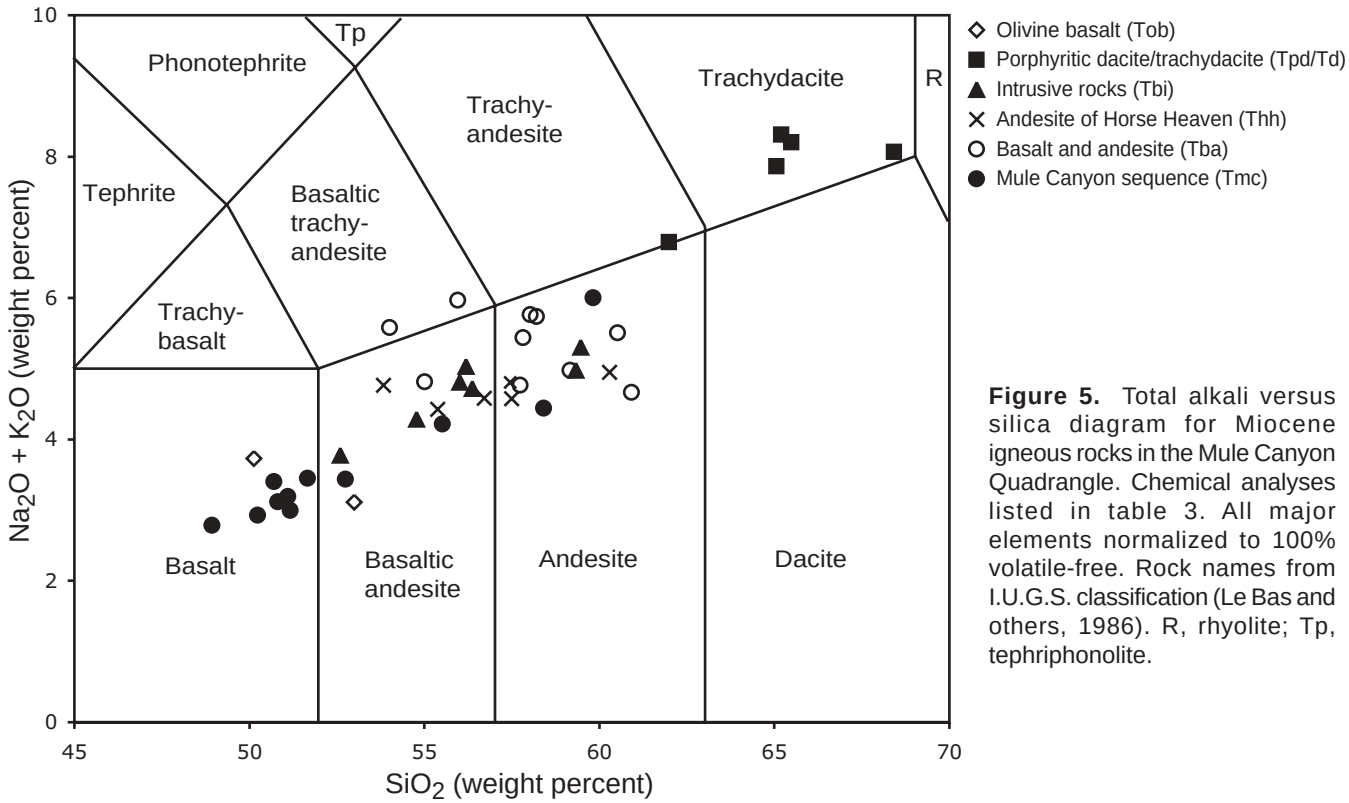

Figure 5. Total alkali versus silica diagram for Miocene igneous rocks in the Mule Canyon Quadrangle. Chemical analyses listed in table 3. All major elements normalized to 100% volatile-free. Rock names from I.U.G.S. classification (Le Bas and others, 1986). R, rhyolite; Tp, tephriphonolite.

14.7±0.2 Ma on lava flows collected in the Mule Canyon Mine area and in the southwestern Sheep Creek Range, respectively (table 1).

The olivine basalt unit is underlain locally by several meters of crystal-lithic rhyolite(?) air-fall tuff, reworked tuff, and tuffaceous sedimentary rocks. This unit is poorly exposed in the Mule Canyon Quadrangle, except in artificial exposures, and it is not shown on the map. These tuffaceous rocks are widely but irregularly distributed along the Argenta and Malpais rims and in the southwestern Sheep Creek Range (Ramelli and others, 2001; John and Wrucke, 2002). Sanidine from an air-fall tuff collected in the southwestern Sheep Creek Range yielded an $^{40}Ar/^{39}Ar$ date of 14.94±0.04 Ma (table 1).

Surficial Deposits

Late Quaternary and older Pleistocene surficial deposits (units Qal, Qay, Qai, Qao, Qc, Qt, Qls, and Qog) cover much of the low areas on the west and east sides of the quadrangle and the west side of the Shoshone Range. Extensive deposits of talus and colluvium cover much of the steep west slopes of the Shoshone Range where the range is capped by mafic lava flows. These deposits commonly mantle contacts between Paleozoic sedimentary rocks, middle Tertiary sedimentary rocks, and Miocene volcanic rocks. Alluvial deposits cover Horse Heaven at the south edge of the quadrangle and the west end of Whirlwind Valley along the east edge of the quadrangle. Older alluvial deposits, distinguished by their height above active drainages, are exposed locally on the west side of the Shoshone Range. The different levels of alluvium may be responses to late Quaternary normal faulting in the adjacent Bateman Spring Quadrangle to the west (Wallace, 1979; Dohrenwend and Moring, 1991).

STRUCTURAL HISTORY

Paleozoic Structural History

The structure of lower Paleozoic rocks in the Mule Canyon Quadrangle is poorly understood. On the basis of regional stratigraphic relations, the lower Paleozoic rocks are part of the Roberts Mountains allochthon and lie in the upper plate of the Roberts Mountains thrust that formed during the Antler orogeny in Late Devonian to Early Mississippian time (Roberts and others, 1958; Roberts, 1964). These deep-water marine sedimentary rocks were thrust tens of kilometers eastward over coeval continental shelf and slope facies carbonate rocks. In the Mule Canyon Quadrangle, the Valmy Formation consists of two thrust sheets that are imbricated with the Slaven Chert by shallow east-dipping faults. Bedding attitudes measured in these rocks generally have shallow eastward dips. Outcrop-scale folds are present in the Slaven Chert, but no map-scale folds have been recognized.

Although fault contacts between the Valmy Formation and the Slaven Chert have shallow east dips subparallel to bedding, middle Tertiary rocks depositionally overlie these rocks and dip moderately to steeply to the east. This relation

Table 3. Chemical analyses of Miocene igneous rocks in the Mule Canyon Quadrangle, northern Shoshone Range, Nevada

Sample No.	98-DJ-17	96-DJ-45	98-DJ-57	96-DJ-46	97-DJ-44	97-DJ-45	96-DJ-48B	99-DJ-9	99-DJ-12	99-DJ-7	96-DJ-49	979-17B	98-DJ-71
Unit	Tob	Tob	Td	Td	Td	Td	Tpd	Tbi	Tbi	Tbi	Tbi	Tbi	Tbi
Lab[1]	2	2	2	2	2	2	1	1	1	1	2	2	1
Major elements (recalculated to 100% volatile free)													
SiO_2 (wt. %)	50.13	52.99	65.06	61.99	65.21	65.49	68.42	52.60	56.36	59.46	54.77	59.33	56.01
Al_2O_3	16.11	15.04	14.05	16.16	13.54	13.81	13.61	16.09	15.32	13.76	14.62	14.35	15.14
TiO_2	1.54	1.36	0.91	0.75	0.91	0.93	0.75	1.12	1.29	1.61	1.56	1.59	1.26
FeO*	11.10	10.67	8.08	6.14	8.06	7.94	6.34	8.87	8.75	10.13	11.25	9.29	9.42
MnO	0.18	0.17	0.13	0.05	0.09	0.08	0.06	0.18	0.19	0.17	0.34	0.18	0.17
CaO	9.60	9.71	2.83	7.27	2.91	2.73	2.12	10.31	8.39	6.39	8.52	6.42	8.43
MgO	6.99	6.46	0.80	0.57	0.73	0.57	0.41	6.71	4.56	2.68	4.14	3.13	4.36
K_2O	0.93	0.76	4.24	3.40	4.63	4.44	4.81	0.90	1.63	2.20	1.35	2.30	1.85
Na_2O	2.79	2.35	3.62	3.39	3.68	3.76	3.25	2.88	3.09	3.11	2.93	2.68	2.95
P_2O_5	0.62	0.51	0.27	0.27	0.25	0.24	0.22	0.34	0.42	0.50	0.52	0.72	0.40
LOI	<0.05	0.77	0.61	0.73	1.62	1.34	1.40	0.93	2.34	1.15	0.99	2.92	0.56
Minor elements (in parts per million)													
Ni	127	74	45	<5	24	<5	3	36	5	2	<5	71	7
Cr	185	na	na	na	na	na	6	200	39	17	na	na	43
Sc	30	28	17	16	14	14.2	8	32	31	28	35	25	32
V	224	203	15	17	18.3	14.2	36	239	244	313	316	253	245
Ba	668	674	1839	1836	1819	2064	1658	409	825	708	698	728	673
Rb	16.0	10.6	130	148	138	140	151	22	56	69	77.1	78.0	46
Sr	441	422	258	255	260	295	253	318	382	294	345	339	346
Zr	153	145	435	456	451	427	386	111	152	194	168	213	154
Y	30	31	61	60	54.8	53.8	56	28	34	39	38	37	32
Nb	12	13	31	36	25	25	25.8	7.1	10.3	13.6	14	15	11.1
Ga	22	19	26	26	24	24	24	19	21	22	21	21	21
Cu	26	23	12	<10	13	11	6	37	16	13	24	18	16
Zn	95	101	98	121	81	72	125	100	110	118	113	141	102
Pb	<5	<5	10	24	31	32	27	5	7	11	8	7	8
Th	1.8	1.9	13.2	13.2	12.0	12.0	17	3	4	6	4.5	4.7	6
La	31.0	25.3	69.3	67.5	64.0	65.0	68.7	18.1	25.6	31.3	25.6	32.0	26.1
Ce	68.0	54.6	134.5	137.5	134.0	130.0	123.6	37.4	51.8	63.2	55.8	77.0	52.0
Pr	7.49	6.36	16.2	15.5	16.3	16.4	14.81	4.64	6.14	7.49	6.50	8.81	6.31
Nd	36.0	29.7	72.7	66.0	63.0	63.0	58.9	20.2	26.0	31.7	29.7	38.0	26.9
Sm	7.50	6.60	13.6	13.7	13.0	13.0	13.0	5.12	6.31	7.81	6.80	7.40	6.48
Eu	1.90	1.69	2.70	2.79	2.62	2.66	2.21	1.46	1.62	1.93	1.70	1.84	1.67
Gd	6.60	5.60	13.4	10.8	11.0	11.0	11.3	5.25	6.18	7.43	6.20	7.70	6.30
Tb	1.10	0.900	2.06	1.80	1.80	1.80	1.75	0.893	1.02	1.23	1.10	1.20	1.03
Dy	6.30	5.50	11.3	10.7	9.90	9.90	10.5	5.55	6.09	7.42	6.30	6.20	6.30
Ho	1.20	1.10	2.23	2.10	2.00	1.90	2.08	1.15	1.25	1.53	1.30	1.40	1.28
Er	3.60	3.30	6.97	6.40	5.90	5.90	5.57	3.13	3.48	4.18	3.90	4.40	3.53
Tm	0.580	0.450	1.05	0.920	0.860	0.850	0.825	0.457	0.500	0.612	0.550	0.630	0.511
Yb	3.50	3.10	6.39	6.40	5.90	5.80	5.21	2.89	3.10	3.84	3.70	3.40	3.22
Lu	0.510	0.490	1.07	1.01	0.880	0.860	0.804	0.456	0.490	0.605	0.580	0.560	0.504
Hf	4.10	3.40	12.6	9.70	10.0	10.0	10.2	3.04	4.00	5.30	4.00	5.60	4.17
Ta	0.670	0.630	2.14	2.05	1.87	1.86	1.51	0.441	0.606	0.871	0.770	0.890	0.636
U	0.50	0.50	4.43	4.50	4.70	4.70	3.76	0.75	1.29	2.17	1.40	2.80	1.29
Cs	<0.5	<0.5	2.3	3.6	3.3	2.7	2.7	0.6	10.3	1.7	9.6	2.2	0.9

[1]Laboratories: 1, GeoAnalytical Lab, Washington State University, Pullman, WA; Major element oxides, Ni, Cr, Sc, V, Ba, Rb, Sr, and Zr by XRF after fusion in LiB_4O_7. Trace elements and REEs by ICP-MS after fusion in LiB_4O_7 (see Johnson and others, 1999). 2, ACTLABS, Inc., Wheat Ridge, CO. Major element oxides, Ba, Sr, Y, Sc, Zr, and V by ICP-ES after fusion with $LiBO_2$. Trace elements and REEs by ICP-MS after fusion with $LiBO_2$. FeO*, Total Fe as FeO; LOI, loss on ignition; na, not analyzed due to contamination during grinding.

continued

Table 3 (*continued*)

Sample No.	99-DJ-61	98-DJ-47	98-DJ-46	98-DJ-56	98-DJ-30	98-DJ-25	96-DJ-41	99-DJ-21	99-DJ-53	98-DJ-29	98-DJ-49	97-DJ-22	97-DJ-38	97-DJ-46
Unit	Tbi	Thh	Thh	Thh	Thh	Tbi (HH)	Thh	Tba	Tba	Tba	Tba	Tba	Tba	Tba
Lab	1	2	2	2	2	2	2	1	1	2	2	2	2	2
Major elements (recalculated to 100% volatile free)														
SiO_2 (wt. %)	56.19	60.30	56.71	57.49	55.38	57.45	53.83	58.02	60.53	55.02	57.75	54.01	55.96	57.83
Al_2O_3	14.48	13.39	14.08	14.69	15.01	14.08	15.74	14.16	13.83	15.60	14.30	16.91	15.88	13.94
TiO_2	1.60	1.52	1.29	1.37	1.41	1.73	1.56	1.76	1.58	1.58	1.59	1.20	1.42	1.65
FeO*	10.34	10.41	10.10	9.24	10.44	10.93	11.12	9.91	9.32	10.75	9.92	9.75	10.37	10.60
MnO	0.18	0.16	0.17	0.18	0.16	0.18	0.17	0.18	0.17	0.16	0.18	0.10	0.11	0.17
CaO	7.61	5.88	7.38	7.72	8.19	6.93	8.14	6.42	6.09	7.15	7.17	7.54	6.26	6.74
MgO	4.00	2.85	5.16	4.31	4.51	3.15	4.06	3.00	2.47	4.25	3.74	4.40	3.03	3.02
K_2O	1.95	1.95	1.62	1.59	1.42	1.76	1.86	2.34	2.54	1.82	1.72	1.93	2.31	2.29
Na_2O	3.08	3.00	2.96	2.99	3.00	3.05	2.91	3.42	2.97	3.00	3.04	3.65	3.65	3.15
P_2O_5	0.57	0.54	0.53	0.42	0.47	0.74	0.61	0.78	0.51	0.68	0.58	0.50	1.00	0.63
LOI	0.76	0.71	0.38	0.49	1.53	2.89	1.99	0.73	1.95	6.33	0.26	1.66	1.28	1.14
Minor elements (in parts per million)														
Ni	3	62	78	49	60	82	15	0	0	67	58	13	20	<5
Cr	27	na	na	na	42	13	na	16	9	63	na	17	14	na
Sc	31	27	28	30	32	27	31	27	33	31	28	28	24	24.8
V	324	302	259	275	267	318	286	338	257	170	307	273	311	293
Ba	773	949	814	798	634	842	730	888	858	682	900	669	825	812
Rb	48	69.5	47.6	48.0	40.0	80.0	59.1	60	83	24.0	52.5	62.0	69.0	61.0
Sr	347	301	325	332	356	356	379	346	315	343	353	318	332	355
Zr	175	183	156	154	151	186	196	204	207	164	166	163	188	179
Y	39	38	34	35	31	36	36	42	41	33	38	29	35	34.7
Nb	12.2	12	10	10	10	12	11	14.1	14.6	11	12	11	12	10
Ga	20	21	20	20	23	22	21	23	19	24	21	20	20	20
Cu	10	22	45	14	26	31	14	11	11	12	11	<10	<10	17
Zn	127	124	102	78	193	154	109	135	121	134	79	126	147	54
Pb	6	13	11	8	18	13	12	9	9	8	7	21	28	20
Th	5	6.6	6.0	5.4	4.6	6.4	5.0	7	7	5.2	6.2	5.7	6.7	5.9
La	30.6	30.3	27.0	26.7	29.0	37.0	27.7	36.5	32.5	31.0	33.0	33.0	42.0	31.0
Ce	61.6	65.7	56.8	57.6	62.0	83.0	57.1	73.6	66.2	71.0	71.5	51.0	63.0	67.0
Pr	7.54	7.56	6.56	6.77	6.73	8.76	7.03	8.98	7.86	8.17	8.19	6.79	8.55	8.56
Nd	32.5	34.7	30.6	31.9	32.0	39.0	31.1	38.1	33.4	38.0	37.8	31.0	39.0	35.0
Sm	7.76	7.20	6.34	6.65	6.60	8.40	7.10	9.12	8.06	7.20	7.50	6.90	8.60	7.70
Eu	1.98	1.63	1.46	1.51	1.63	2.00	1.67	2.21	2.00	1.71	1.70	1.60	1.92	1.79
Gd	7.28	7.29	6.38	6.84	6.20	7.60	6.10	8.35	7.64	7.20	7.61	6.60	7.70	7.00
Tb	1.20	1.19	1.06	1.12	1.10	1.20	1.10	1.36	1.270	1.20	1.21	1.10	1.20	1.10
Dy	7.34	6.68	5.81	6.13	6.30	7.00	6.20	8.21	7.81	6.40	6.68	6.10	7.00	6.30
Ho	1.51	1.37	1.17	1.24	1.20	1.40	1.20	1.67	1.61	1.30	1.29	1.20	1.40	1.20
Er	4.02	4.18	3.55	3.76	3.60	4.10	3.70	4.45	4.34	4.20	4.01	3.60	4.10	3.60
Tm	0.578	0.614	0.526	0.585	0.590	0.600	0.520	0.641	0.635	0.670	0.622	0.550	0.620	0.520
Yb	3.58	3.86	3.28	3.43	3.60	3.70	3.20	3.97	3.96	3.80	3.68	3.40	3.70	3.50
Lu	0.574	0.632	0.545	0.584	0.500	0.590	0.530	0.626	0.622	0.540	0.614	0.540	0.600	0.520
Hf	4.90	5.65	4.75	4.60	4.20	5.10	4.60	5.59	5.74	5.00	4.91	4.40	4.80	4.40
Ta	0.753	0.856	0.668	0.672	0.680	0.770	0.71	0.860	0.973	0.71	0.77	0.66	0.76	0.70
U	1.48	2.34	1.85	1.59	1.30	1.70	1.40	1.84	2.65	1.30	1.84	1.70	1.90	1.70
Cs	1.1	1.5	1.0	1.5	0.8	<0.5	1.5	1.0	2.3	<0.5	1.0	0.6	0.8	1.4

continued

Table 3 (*continued*)

Sample No.	96-DJ-42	96-DJ-43	97-DJ-47	97-DJ-23	99-DJ-13	97-DJ-48	98-DJ-50	98-DJ-26	98-DJ-27	99-DJ-5	98-DJ-79	99-DJ-3	FW CPU	MC 282-482
Unit	Tba	Tba	Tba	Tmc	Tmc	Tmc	Tmc	Tmc	Tmc	Tmc	Tmc	Tmc	Tmc	Tmc
Lab	2	2	2	1	1	2	2	2	2	1	1	1	2	2
Major elements recalculated to 100% volatile free														
SiO_2 (wt. %)	59.17	60.93	58.21	50.70	51.67	52.75	55.52	59.83	58.41	50.81	51.10	50.23	51.17	48.93
Al_2O_3	14.06	13.22	13.79	16.41	16.10	15.38	14.66	15.42	17.04	16.72	18.54	18.02	19.76	19.97
TiO_2	1.53	1.42	1.65	1.09	1.06	1.09	1.60	1.49	1.66	1.09	1.04	0.97	0.95	0.97
FeO*	10.46	9.76	11.36	9.91	9.62	9.83	10.61	8.39	6.94	9.14	7.19	8.98	8.76	9.03
MnO	0.16	0.15	0.15	0.18	0.18	0.19	0.16	0.15	0.14	0.16	0.14	0.16	0.11	0.16
CaO	6.62	6.32	5.73	10.68	10.43	10.47	8.27	5.60	6.72	10.70	13.62	11.49	11.03	11.59
MgO	2.35	2.90	2.68	7.32	7.24	6.54	4.42	2.45	3.87	7.99	4.90	6.96	4.97	6.32
K_2O	2.10	2.02	2.65	0.68	0.71	0.81	1.38	2.53	1.42	0.53	0.46	0.36	0.37	0.38
Na_2O	2.88	2.64	3.08	2.72	2.74	2.62	2.84	3.47	3.01	2.58	2.73	2.57	2.62	2.40
P_2O_5	0.68	0.64	0.69	0.30	0.26	0.31	0.55	0.67	0.77	0.28	0.27	0.26	0.26	0.25
LOI	0.91	1.14	3.04	<0.05	0.83	2.69	2.58	2.66	9.05	3.52	5.00	1.75	5.82	9.89
Minor elements (in parts per million)														
Ni	<5	<5	40	52	45	87	67	58	65	46	38	41	61	73
Cr	na	na	na	137	153	na	na	na	na	155	138	146	130	128
Sc	28	26	24	32	33	29.9	33	21	21	37	35	35	30	31
V	200	178	289	247	234	244	276	211	246	236	238	221	200	199
Ba	821	739	865	358	347	388	759	1174	965	342	321	263	269	147
Rb	54.4	45.4	65.0	11	17	18.0	45.7	96.0	50.0	8	5	10	4.3	3.7
Sr	347	322	354	328	308	340	311	437	473	282	363	339	382	341
Zr	188	175	189	94	96	96.8	149	221	233	88	89	83	73	65
Y	36	35	33.3	27	27	24.3	37	33	35	27	27	25	19	20
Nb	14	14	10	7	6.1	6	9	14	14	5.9	5.9	5.3	5	4
Ga	21	21	20	16	19	17	20	24	25	19	18	19	20	17
Cu	<10	<10	16	62	39	51	29	17	16	32	33	41	30	36
Zn	100	37	76	97	95	31	111	205	165	98	92	91	111	105
Pb	18		20	0	1	10	9	24	9	0	4	0	<5	<5
Th	6.0	6.0	6.0	4	2	2.1	5.1	6.5	7.1	2	2	3	0.9	0.9
La	31.3	31.4	31.0	14.2	14.5	15.0	25.1	42.0	44.0	12.5	12.2	12.0	12.0	11.0
Ce	67.7	68.6	69.0	29.7	29.6	34.0	54.9	89.0	95.0	26.5	25.6	25.2	27.0	26.0
Pr	7.67	7.79	8.73	3.81	3.65	4.52	6.56	9.89	10.60	3.42	3.32	3.25	3.10	2.87
Nd	35.2	35.8	36.0	17.1	16.3	19.0	31.0	46.0	48.0	15.3	15.0	14.5	16.0	13.0
Sm	7.80	7.80	7.80	4.54	4.28	4.60	6.54	8.70	9.20	4.15	4.09	3.86	3.60	3.30
Eu	1.83	1.79	1.82	1.37	1.32	1.19	1.53	1.80	1.96	1.25	1.26	1.20	1.04	1.11
Gd	6.70	6.70	7.10	4.77	4.65	4.40	6.83	7.90	8.50	4.47	4.32	4.15	3.50	3.30
Tb	1.10	1.10	1.10	0.816	0.809	0.800	1.16	1.30	1.40	0.776	0.741	0.717	0.700	0.600
Dy	6.50	6.50	6.30	5.12	5.05	4.40	6.64	6.70	7.10	4.86	4.72	4.54	4.00	3.70
Ho	1.30	1.30	1.20	1.08	1.08	0.900	1.34	1.30	1.40	1.02	0.993	0.953	0.800	0.800
Er	3.80	4.00	3.60	2.97	3.05	2.60	4.08	4.20	4.30	2.85	2.73	2.70	2.50	2.40
Tm	0.540	0.550	0.510	0.438	0.437	0.390	0.602	0.640	0.670	0.411	0.398	0.385	0.410	0.350
Yb	3.50	3.70	3.40	2.73	2.75	2.60	3.63	3.70	3.80	2.57	2.50	2.42	2.60	2.30
Lu	0.540	0.580	0.490	0.429	0.435	0.380	0.609	0.530	0.540	0.410	0.400	0.385	0.370	0.360
Hf	4.10	4.30	4.50	2.60	2.57	2.60	4.62	6.30	6.70	2.33	2.31	2.21	2.10	1.80
Ta	0.72	0.77	0.72	0.336	0.332	0.36	0.61	0.84	0.88	0.292	0.289	0.282	0.29	0.23
U	1.00	0.90	1.70	0.32	0.49	0.70	1.19	1.40	1.50	0.31	0.30	0.290	.30	0.30
Cs	0.7	<0.5	2.3	0.1	0.7	0.9	1.3	2.3	3.0	2.1	0.0	0.9	<0.5	<0.5

continued

is best displayed near the southwest corner of the quadrangle where the basal vitrophyre of the Caetano Tuff dips 50–60° to the east subparallel to the steeply dipping contact between the Caetano Tuff and the underlying Valmy Formation (see cross sections). On one hand, if the basal Caetano Tuff contact originally was near horizontal, then these relations suggest that the "thrust" faults might have originated as moderately to steeply west-dipping faults and were rotated, along with the tuff, to their present shallow east dips by late Cenozoic faulting and tilting. On the other hand, the exposed Caetano Tuff may have been deposited along the side of a north-trending paleovalley, and part of its steep east dip may be primary. For example, the Caetano Tuff and other Oligocene tuffs in nearby ranges are known to have filled paleovalleys (e.g., Emigrant Pass area, Henry and Ressel, 2000; McCoy Mine area, Marcus Johnston, oral commun., 2001; Marigold Mine area, Doug McGibbon, oral commun., 2001). Assuming a primary 20° to 30° east dip for the exposed Caetano Tuff, untilting the tuff restores the faults to shallow westerly dips that are more consistent with an origin as east-directed thrust faults that formed during the Paleozoic.

Middle Tertiary Tilting and Faulting

Variable, but moderate to steep, east to east-southeast dips of the Caetano Tuff and locally in the overlying middle Tertiary sedimentary rocks suggest a period of extensional faulting and tilting between about 34 and 16 Ma (Wallace and John, 1998). As noted above, part of the steep dip of the Caetano Tuff may be primary due to deposition in a paleovalley. However, the overlying sedimentary rocks also generally dip 25° to 55° east to southeast, more steeply than the middle Miocene volcanic rocks, suggesting that east to southeast tilting occurred prior to the middle Miocene. The middle Tertiary sedimentary rocks generally have shallower dips than the exposed Caetano Tuff, however, suggesting either that there were two discrete periods of faulting and tilting, one prior to and one following deposition of the sedimentary rocks, or more likely, that the sedimentary rocks were deposited during faulting and basin formation. The latter relation also is suggested by generally fining upward textures of the sedimentary rocks from coarse sedimentary breccia and conglomerate near the base of the sequence to finely laminated mudstone and lacustrine limestone near the top. This tilting may be related to extensional faulting and formation of a 75-km-long, north- to northwest-elongated basin along the axis of the subsequent northern Nevada rift between the Humboldt River and the Simpson Park Range (John and others, 2000). Middle Tertiary tilting also has been reported in the Ivanhoe district 65 km to the north (Wallace and John, 1998; Wallace, 2003a) and in the Emigrant Pass area 35 km to the northeast (Henry and Faulds, 1999), but the regional extent and exact timing of this event are unknown.

Middle Miocene Crustal Extension, Faulting, and Formation of the Northern Nevada Rift

In northern Nevada, the middle Miocene was marked by the beginning of block faulting related to regional crustal extension, widespread bimodal basalt-rhyolite magmatism, and formation of the northern Nevada rift. The northern Nevada rift is a major geophysical feature that extends about 500 km from southeast Oregon to southern Nevada along a N10–20°W trend (Zoback and Thompson, 1978; Blakely and Jachens, 1991; Zoback and others, 1994; John and others, 2000). It is marked by a prominent narrow positive aeromagnetic anomaly that corresponds, in part, to middle Miocene mafic igneous rocks. John and others (2000, fig. 5) showed that the structural boundaries of the rift are wider than the aeromagnetic anomaly and that the rift generally narrows to the south.

At the latitude of the Mule Canyon Quadrangle, the structural margins of the northern Nevada rift are about 19 km apart, and the rift consists of several blocks separated by north-northwest-striking high-angle faults (fig. 2; Struhsacker, 1980; John and others, 2000). The western block lies in central part of the Mule Canyon Quadrangle, is about 3 km wide, and exposes the oldest rift-related rocks, the Mule Canyon sequence, the andesite of Horse Heaven, and an extensive set of north-northwest-striking mafic dikes. Here, the aeromagnetic anomaly is about 3 km wide and coincides with the western part of the structural rift and to the older set of mafic dikes in the western third of the quadrangle.

The central part of the rift lies between the Muleshoe fault on the west and the Dunphy Pass fault on the east (fig. 2). South of the Argenta Rim, it is filled by much thicker sequences of the middle Miocene rocks than other parts of the rift (section B–B´ and fig. 3; John and others, 2000). Here, the central part of the rift is filled by younger middle Miocene rocks (porphyritic dacite, trachydacite, and olivine basalt units), as well as by thick sequences of the early mafic flow units. Geothermal wells drilled near Beowawe Hot Springs just east of the quadrangle show that the middle Miocene volcanic rocks in the central part of the rift are as much as 1.2 km thick and that numerous diabase dikes or sills are present in the underlying lower Paleozoic rocks (fig. 3; Struhsacker, 1980; Cole and Ravinsky, 1984). Farther north on the north side of the Argenta Rim, the middle Miocene volcanic rock units have a relatively constant total thickness of about 400–500 m, much less than the total thickness of the same units on the south side of Whirlwind Valley (fig. 3). This suggests that northeast-striking faults must have cut across the central part of the rift in this area to form a box-like graben (John and others, 2000). The southern bounding fault probably lies on the south side of the Malpais rim between the south side of Horse Heaven and the Fire Creek deposit (fig. 2) and confines the lower part of middle Miocene volcanic rocks (Mule Canyon sequence) to its north side. The northern bounding fault must lie between Whirlwind Valley and the north edge of the Argenta Rim (fig. 2 and section A–A´).

The Muleshoe fault is a major intrarift fault that runs the length of the Mule Canyon Quadrangle, strikes N5–10°W, dips 55–60° east, and, along much of its length, juxtaposes much thicker sequences of middle Miocene rocks to the east against thinner sequences to the west (section B–B´ and fig. 3; John and others, 2000).

Numerous other north- to northwest- and northeast-striking, high-angle faults with small amounts of displacement were active during middle Miocene magmatism and rift formation. These faults are well exposed in the open pits at the Mule Canyon Mine (Newmont Gold Co., 1999; John and others, 2000, 2003) and along both the Argenta and Malpais rims (Struhsacker, 1980; D.A. John, unpub. mapping, 1999). Dikes that fed lava flows in the Mule Canyon sequence and the andesite of Horse Heaven intruded many of the north-northwest-striking faults.

Late Cenozoic Structure

The northern Shoshone Range is a northeast-trending, gently southeast-tilted horst formed by late Cenozoic basin-and-range faulting. The range is bounded on its west and north sides by north- to northeast-striking fault zones with late Quaternary displacement that form the Reese River and Humboldt River valleys (fig. 2; Wallace, 1977; Dohrenwend and Moring, 1991). Modeling of gravity data on the northwest side of the range suggests that total offset on the east side of Reese River Valley is about 4.3 km (John and others, 2000).

The Argenta and Malpais rims are northeast- to east-northeast-trending fault blocks that were formed by late Miocene to Quaternary faulting (fig. 2). The faulting produced gentle southeast tilting of the middle Miocene rocks (Zoback, 1979; Struhsacker, 1980; Zoback and others, 1994). A series of steep north-dipping faults bound the north sides of both blocks, and nearly 1 km of topographic relief is present on the Argenta Rim. The Humboldt River and Whirlwind Valleys formed on the down-dropped north sides of these faults. Horse Heaven, at the south edge of the quadrangle, formed at the intersection of the east-northeast-striking, north-dipping Corral Canyon fault with the gently southeast-tilted crest of the north end of the Shoshone Range (fig. 2).

The Malpais and Argenta rims were formed by east-northeast-striking, left-lateral oblique-slip faults that reflect a change in the regional stress regime that began after 10 Ma (Zoback and others, 1981, 1994). Between about 10 to 6 Ma, the least principal stress direction rotated approximately 40° clockwise, and the northeast- to east-northeast-striking faults bounding the Argenta and Malpais rims, as well as the south end of the Sheep Creek Range, began to form. Both the structural and aeromagnetic expressions of the northern Nevada rift are offset about 4 km in a left lateral sense by the east-northeast-striking faults that bound the Argenta Rim and the south side of the Sheep Creek Range (Zoback and others, 1994). The Muleshoe fault appears to be offset about 500 m left laterally by the Corral Canyon fault. The Beowawe geothermal system is along the Malpais fault that bounds the north side of the Malpais rim (fig. 2). Zoback and others (1994) showed that left-lateral oblique-slip displacement along the northeast-striking faults is consistent with regional WNW-ESE crustal extension.

MINERAL DEPOSITS

Two types and ages of mineral deposits are present in the Mule Canyon Quadrangle: sedimentary barite deposits in the Devonian Slaven Chert (Papke, 1984; Long, 1984; Jewell and Stallard, 1991) and epithermal gold-silver deposits in the middle Miocene igneous rocks (Thomson and others, 1993; Serenko, 1995; Newmont Gold Co., 1999; John and Wallace, 2000; John and others, 2003).

Barite Deposits

Numerous barite prospects, small mines, and the much larger Miller (D.A.) Mine are in the Mule Canyon Quadrangle (fig. 4). In addition, the Argenta Mine, one of the largest barite mines in Nevada, lies just north of the quadrangle (fig. 4) and several other large barite mines are in nearby ranges (Papke, 1984). All of the barite mines and prospects are in Devonian Slaven Chert that contains irregular beds of barite interbedded in chert and less abundant argillite and shale.

The Miller (D.A.) Mine near the southwest corner of the quadrangle is the largest barite deposit in the quadrangle. Most production was in the 1960s, with some additional production in the early 1980s (Papke, 1984); the mine recently reopened in 2002. Barite is present in three, more-or-less conformable bodies over a stratigraphic interval of about 100 m. The barite bodies are about 3–10 m thick and are separated by chert and argillite of similar thickness. The barite bodies have strike lengths of about 200 m. Limestone lenses commonly underlie the barite-bearing zone. Barite is typically very thin bedded, medium dark-gray to light brownish-gray, and fine-grained. Thin beds of gossanous Fe-oxide minerals containing highly anomalous zinc contents are common near the barite bodies. Mitchell (1977), Papke (1984), and Jewell and Stallard (1991) provide more detailed descriptions of the deposit.

Epithermal Au-Ag Deposits

Epithermal gold-silver ore was discovered in the Mule Canyon area in 1986 by Gold Fields Mining Corp. (Thomson and others, 1993). Exploration and drilling in the area by Gold Fields, and later by Santa Fe Pacific Gold Co. after it purchased Gold Fields in 1993, continued through 1996, resulting in the definition of six economic ore zones in a north-northwest-elongated zone about 2.5 km long and 0.6 km wide (fig. 4). Several of the ore zones cropped out. The combined orebodies contained about 9 million tons of ore at an average grade of 0.111 oz Au/ton and a cut-off grade of 0.097 oz Au/ton. About 85% of the ore was unoxidized. Other drilled resources in the Far West and Section 9 zones (fig. 4), west and southwest of the economic ore bodies, respectively, increased the total Au resources in the area to

about 1.3 million oz Au. Mining began in December 1996 and continued until August 2000, when operations ceased due to low gold prices. The mine briefly reopened between May and September 2002. Less than half of the pre-mining reserves were mined prior to the cessation of large-scale mining in 2000. The mine was acquired by Newmont Mining Co. in early 1997 when they purchased Santa Fe Pacific Gold Co., and Newmont presently owns the property.

Mule Canyon is a shallowly formed, low-sulfidation deposit hosted by mafic lava flows and dikes of the Mule Canyon sequence (Thomson and others, 1993; Serenko, 1995; Newmont Gold Co., 1999; John and Wallace, 2000; John and others, 2003). Ore has tight structural controls and is present in narrow, north-northwest-striking, steeply dipping faults, breccia zones, and brecciated margins of mafic dikes that intruded faults. Most ore is associated with silicification, potassium metasomatism, and intense sulfidation. Ore forms narrow silica-adularia veins and stockwork zones, silica-adularia cemented breccias, and local disseminations in permeable units (e.g., vesicular flow tops). Silica phases, mostly opal and chalcedony, locally replaced bladed carbonate minerals. Gold is present both in electrum and in arsenopyrite and arsenic-rich overgrowths on pyrite and marcasite. Silver is present in electrum and in silver sulfides and selenides. Pyrite, marcasite, and arsenopyrite are abundant in most ore and altered wall rock. Stibnite is the only other abundant sulfide mineral in ore. Hydrothermal alteration distant from major fluid conduits generally is weak, and large zones of steam-heated acid-sulfate alteration did not overlie zones of ore formation. John and others (2000) reported a $^{40}Ar/^{39}Ar$ date of 15.59±0.04 Ma for adularia from a gold-bearing quartz-adularia vein from the South pit (A3, table 1; fig. 4).

Several other zones of hydrothermal alteration and low-grade gold-silver- mineralized rock have been discovered along the west side of the northern Nevada rift in the Mule Canyon Quadrangle and farther south in the Fire Creek Mine area (fig. 2). These areas include the head of Water Canyon along the west end of the Argenta Rim at the north end of the Mule Canyon Quadrangle and in the adjacent Argenta Quadrangle and south of the Mule Canyon Mine near the road that crosses the crest of the range in the center of the quadrangle (fig. 4). The Fire Creek deposit is described briefly by John and Wallace (2000). All known mineralized occurrences are hosted by rocks in the Mule Canyon sequence and the andesite of Horse Heaven and are controlled by north- to north-northwest-striking faults.

ACKNOWLEDGMENTS

We want to thank Eric Saderholm and Jon Brummer for access to the Mule Canyon Mine and lots of information and stimulating discussion about the Mule Canyon area and the northern Nevada rift. Eric also provided a copy of Tom Chapin's unpublished geologic map of the mine area. Bob Fleck provided the $^{40}Ar/^{39}Ar$ dates, and Chuck Holdsworth prepared the samples for dating. Kelly Cluer provided fossil data and information of the Paleozoic stratigraphy in the northern Shoshone Range. Anita Harris identified several conodont samples, and Stan Finney identified several graptolite samples. Alan Ramelli provided information and suggestions about surficial map units along the west side of the quadrangle. Reviews by Ted Theodore, Alan Wallace, Chris Henry, Eric Struhsacker, and Alan Ramelli improved the presentation.

REFERENCES

Blakely, R.J., and Jachens, R.C., 1991, Regional study of mineral resources in Nevada—Insights from three-dimensional analysis of gravity and magnetic anomalies: Geological Society of America Bulletin, v. 103, p. 795–803.

Cole, D.R., and Ravinsky, L.I., 1984, Hydrothermal alteration zoning in the Beowawe geothermal system, Eureka and Lander Counties, Nevada: Economic Geology, v. 79, p. 759–767.

Dohrenwend, J.C., and Moring, B.C., 1991, Reconnaissance photogeologic map of young faults in the Winnemucca 1° by 2° quadrangle, Nevada: U.S. Geological Survey Miscellaneous Field Studies Map MF-2175, scale 1:250,000.

Gilluly, J., and Gates, O., 1965, Tectonic and igneous geology of the northern Shoshone Range, Nevada: U.S. Geological Survey Professional Paper 465, 153 p.

Gilluly, J., and Masursky, H., 1965, Geology of the Cortez quadrangle, Nevada: U.S. Geological Survey Bulletin 1175, 117 p.

Henry, C.D., and Faulds, J.E., 1999, Geologic map of the Emigrant Pass Quadrangle, Nevada: Nevada Bureau of Mines and Geology Open-File Report 99-9, scale 1:24,000, 20 p. text.

Henry, C.D., and Ressel, M.W., 2000, Interrelation of Eocene magmatism, extension, and Carlin-type gold deposits in northeastern Nevada, *in* Lageson, D.R., Peters, S.G., and Lahren, M.M., eds., Great Basin and Sierra Nevada: Boulder, Colorado, Geological Society of America Field Guide 2, p. 165–187.

House, P.K., Ramelli, A.R., and Wrucke, C.T., 2001, Geologic map of the Battle Mountain Quadrangle, Lander County, Nevada: Nevada Bureau of Mines and Geology Map 130, scale 1:24,000.

House, P.K., Ramelli, A.R., Wrucke, C.T., and John, D.A., 2000, Geologic map of the Argenta Quadrangle, Nevada: Nevada Bureau of Mines and Geology Open-File Report 2000-7, scale 1:24,000.

Jewell, P.W., and Stallard, R.F., 1991, Geochemistry and paleoceanographic setting of central Nevada bedded barites: Journal of Geology, v. 99, p. 151–170.

John, D.A., Hofstra, A.H., Fleck, R.J., Brummer, J.E., and Saderholm, E.C., 2003, Geologic setting and genesis of the Mule Canyon low-sulfidation epithermal gold-silver deposit, north-central Nevada: Economic Geology, v. 98, p. 425–463.

John, D.A., and Wallace, A.R., 2000, Epithermal gold-silver mineral deposits related to the northern Nevada rift, *in* Cluer, J.K., Price, J.G., Struhsacker, E.M., Hardyman, R.F., and Morris, C.L., eds., Geology and Ore Deposits 2000: The Great Basin and Beyond: Geological Society of Nevada Symposium Proceedings, Reno, May 15–18, 2000, p. 155–175.

John, D.A., Wallace, A.R., Ponce, D.A., Fleck, R.B., and Conrad, J.E., 2000, New perspectives on the geology and origin of the northern Nevada Rift, *in* Cluer, J.K., Price, J.G., Struhsacker, E.M., Hardyman, R.F., and Morris, C.L., eds., Geology and Ore Deposits 2000: The Great Basin and Beyond: Geological Society of Nevada Symposium Proceedings, Reno, May 15–18, 2000, p. 127–154.

John, D.A., and Wrucke, C.T., 2002, Geologic map of the Izzenhood Spring quadrangle, Lander County, Nevada: U.S. Geological Survey Geologic Investigations Series Map I-2668, scale 1:24,000.

Johnson, D.M., Hooper, P.R., and Conrey, R.N., 1999, XRF analysis of rocks and minerals for major and trace elements on a single low dilution Li-tetraborate fused bead: Advances in X-ray Analysis, v, 41, p. 843–867

Le Bas, M.J., LeMaitre, R.W., Streckeisen, A., and Zanettin, B., 1986, A chemical classification of volcanic rocks based on the total alkali-silica diagram: Journal of Petrology, v. 27, p. 745–750.

Long, J.R., 1984, Field Trip 9. Road log/trip guide: Mountain Springs, Greystone, Argenta mines, *in* Johnson, J.L., ed., Exploration for ore deposits of the North American Cordillera; field trip guidebook: Association of Exploration Geochemists, Reno, p. 1–4.

Mitchell, A.W., 1977, Geology of some bedded barite deposits, north central Nevada [MS thesis]: University of Nevada, Reno, 58 p.

Newmont Gold Co., 1999, Mule Canyon mine, *in* Kizis, J.A., Jr., ed., Low-sulfidation gold deposits in northern Nevada: Reno, Geological Society of Nevada, 1999 Spring Field Trip Guidebook, Special Publication No. 29, p. 189–203.

Noble, P.J., 2000, Revised stratigraphy and structural relationships in the Roberts Mountains allochthon of Nevada (USA) based on radiolarian cherts, *in* Cluer, J.K., Price, J.G., Struhsacker, E.M., Hardyman, R.F., and Morris, C.L., eds., Geology and Ore Deposits 2000: The Great Basin and Beyond: Geological Society of Nevada Symposium Proceedings, Reno, May 15–18, 2000, p. 439–449.

Papke, K.G., 1984, Barite in Nevada: Nevada Bureau of Mines and Geology Bulletin 98, 125 p.

Peters, S.G., 2003, Geologic map of the Bobs Flat Quadrangle, Elko County, Nevada: Nevada Bureau of Mines and Geology Map 138, scale 1:24,000.

Ramelli, A.R., House, P.K., Wrucke, C.T., and John, D.A., 2001, Geologic map of the Stony Point Quadrangle, Nevada: Nevada Bureau of Mines and Geology Map 131, scale 1:24,000.

Roberts, R.J., 1964, Stratigraphy and structure of the Antler Peak quadrangle, Humboldt and Lander Counties, Nevada: U.S. Geological Survey Professional Paper 459-A, 93 p.

Roberts, R.J., Ferguson, H.G., Gilluly, J., and Hotz, P.E., 1958, Paleozoic rocks of north-central Nevada: American Association of Petroleum Geologists, v. 42, p. 2813–2857.

Serenko, T.J., 1995, Nature of gold mineralization at Mule Canyon, Lander County, Nevada, U.S.A.: Transactions of the Institute of Mining and Metallurgy, v. 104, section B, p. B99–B110.

Stewart, J.H., and Carlson, J.E., 1976, Geologic map of north-central Nevada: Nevada Bureau of Mines and Geology Map 50, scale 1:250,000.

Stewart, J.H., and McKee, E.H., 1977, Geology and mineral deposits of Lander County, Nevada, *with a section on* Mineral deposits by H.K. Stager: Nevada Bureau of Mines and Geology Bulletin 88, 106 p.

Struhsacker, E.M., 1980, The geology of the Beowawe geothermal system, Eureka and Lander Counties, Nevada: University of Utah Research Institute, Earth Science Laboratory Division Report ESL-37, 78 p.

Theodore, T.G., Moring, B.C., Chadwick, T., Dobak, P.J., and Cluer, J.K., in prep., Geologic map of the Santa Renia Fields Quadrangle, Elko County, Nevada: Nevada Bureau of Mines and Geology Map Series, scale 1:24,000.

Theodore, T.G., Moring, B.C., Harris, A.G., Armstrong, A.K, and Finney, S.C., 2003, Geologic map of the Beaver Peak Quadrangle, Elko County, Nevada: Nevada Bureau of Mines and Geology Map 143, scale 1:24,000.

Thomson, K., Brummer, J.E., Caldwell, D.A., McLachlan, C.D., and Schumacher, A.L., 1993, Geology and geochemistry of the Mule Canyon gold deposit, Lander County, Nevada: Society for Mining, Metallurgy, and Exploration, Inc., Preprint 93-271, 10 p.

Wallace, A.R., 1990, Geologic map of the Jake Creek Mountain quadrangle, Elko County, Nevada: U.S. Geological Survey Geologic Quadrangle Map GQ-1672, scale 1:24,000.

Wallace, A.R., 2003a, Geologic map Willow Creek Reservoir Quadrangle, Elko County: Nevada Bureau of Mines and Geology Map 135, scale 1:24,000.

Wallace, A.R., 2003b, Willow Creek Reservoir SE Quadrangle, Elko, Eureka, and Lander counties: Nevada Bureau of Mines and Geology Map 136, scale 1:24,000.

Wallace, A.R., and John, D.A., 1998, New studies of Tertiary volcanic rocks and mineral deposits, northern Nevada rift, *in* Tosdal, R.M., ed., Contributions to the gold metallogeny of northern Nevada: U.S. Geological Survey Open-File Report 98-338, p. 264–278.

Wallace, R.E., 1977, Profiles and ages of young fault scarps, north-central Nevada: Geological Society of America Bulletin, v. 88, p. 1267–1281.

Wallace, R.E., 1979, Map of young fault scarps related to earthquakes in north-central Nevada: U.S. Geological Survey Open-File Report 79-1554, 2 sheets.

Wrucke, C.T., and Silberman, M.L., 1975, Cauldron subsidence of Oligocene age at Mount Lewis, northern Shoshone Range, Nevada: U.S. Geological Survey Professional Paper 876, 19 p.

Zoback, M.L., 1979, A geologic and geophysical investigation of the Beowawe geothermal area, north-central Nevada: Stanford University Publications, Geological Sciences, v. 16, 79 p.

Zoback, M.L., Anderson, R.E., and Thompson, G.A., 1981, Cainozoic evolution of the state of stress and style of tectonism of the Basin and Range province: Philosophical Transactions of the Royal Society of London, v. A300, p. 407–434.

Zoback, M.L., McKee, E.H., Blakely, R.J., and Thompson, G.A., 1994, The northern Nevada rift: Regional tectonomagmatic relations and middle Miocene stress direction: Geological Society of America Bulletin, v. 106, p. 371–382.

Zoback, M.L., and Thompson, G.A., 1978, Basin and Range rifting in northern Nevada: Clues from a mid-Miocene rift and its subsequent offsets: Geology, v. 6, p. 111–116.